

SUBMILLIMETER PHOTOMETRY AND DISK MASSES OF T TAURI DISK SYSTEMS

FRED C. ADAMS,¹ JAMES P. EMERSON,² AND GARY A. FULLER³*Received 1989 July 21; accepted 1990 January 9*

ABSTRACT

We present submillimeter photometric measurements of T Tauri stars which are suspected of having circumstellar disks. The sources T Tau, HL Tau, DG Tau, HK Tau, DO Tau, GM Aur in Taurus-Auriga and VSSG 23 in Ophiuchus were detected. For the most luminous sources, detections were obtained at all of the observed wavelengths (1100, 800, 600, 450, and 350 μm); for the less luminous sources, detections were obtained only at the longer wavelengths (usually 800 and 1100 μm). We interpret the submillimeter emission as arising from circumstellar disks and we derive estimates for the disk mass M_D which are found to be in the range $0.05 M_\odot \leq M_D \leq 1.0 M_\odot$ (for an opacity law of the form $\kappa_\nu \propto \nu^2$ at low frequencies). These disk masses are larger than the “minimum-mass” solar nebula and suggest that planets can form in these systems.

Subject headings: infrared: spectra — spectrophotometry — stars: accretion — stars: circumstellar shells — stars: pre-main-sequence

I. INTRODUCTION

When newly formed low-mass stars (T Tauri stars) first appear in the H-R diagram, they often have infrared excesses in their spectral energy distributions (see, e.g., Mendoza 1966, 1968; Rydgren and Zak 1987). These sources have been well observed in the near- and mid-infrared (see Rydgren *et al.* 1984 for a compilation of data for sources in the Taurus-Auriga region). At longer wavelengths, the infrared excess of these sources have been observed by the *IRAS* satellite for $12 \mu\text{m} \leq \lambda \leq 100 \mu\text{m}$ (see, e.g., Rucinski 1985; Cohen, Emerson, and Beichman 1989, hereafter CEB). However, before the new generation of submillimeter telescopes became operational, very little data existed for these objects in the spectral region between 100 μm and 1 mm. Hence, the first objective of this present work is to fill in this gap by measuring the spectra in the submillimeter regime. Specifically, we present broad-band photometric observations in the wavelength range 1100 μm to 350 μm for sources in both the Taurus and Ophiuchus molecular clouds. Related work has been done recently by Weintraub, Sandell, and Duncan (1989, hereafter WSD) and by Beckwith *et al.* (1990).

The most likely explanation for the observed excess infrared emission in these systems is the presence of circumstellar disks (see, e.g., Bertout, Basri, and Bouvier 1988; Kenyon and Hartmann 1987; Adams, Lada, and Shu 1987, 1988). Further evidence for circumstellar disks in T Tauri systems is provided by optical polarization studies (see Elsasser and Staude 1978) and by the finding that only blueshifted line emission can be observed in the winds of many of these sources (Edwards *et al.* 1987; see also Hartmann and Raymond 1989). In addition, near-infrared speckle observations (e.g., Beckwith *et al.* 1984), direct near-infrared imaging (Grasdalen *et al.* 1984), and kinematic studies using CO emission (Beckwith *et al.* 1986; Sargent and Beckwith 1987) also indicate the presence of circumstellar disks.

Although there is considerable variation from source to source, the general properties of these putative disks can be summarized as follows: The spectral energy distributions in the

infrared are nearly power laws (see Rucinski 1985; Rydgren and Zak 1987), which implies that the disk temperature distributions are also nearly power-laws. The total disk luminosity L_D can be large, i.e., comparable to the stellar luminosity L_* (see, e.g., Bertout, Basri, and Bouvier 1988; Adams, Lada, and Shu 1988, hereafter ALS); however, direct estimates of the intrinsic disk luminosity are complicated by the possibility of disk flaring (see Kenyon and Hartmann 1987). CEB have assessed the overall energetics of 72 T Tauri stars in the Taurus-Auriga region in terms of their ratios of bolometric L_{bol} to stellar L_* luminosity (see also Strom *et al.* 1988 for a different method of addressing the same problem). CEB estimate that at least $\frac{1}{3}$ of the stars must have disks, based on the large values of the ratio L_{bol}/L_* ; in addition, they find that stars with strong [O I] emission tend to have the largest luminosity ratios, up to ~ 4 . Such large values of L_{bol}/L_* suggest the presence of active (i.e., self-luminous) accretion disks. The expected radial size of T Tauri disks is $R_D \sim 100 \text{ AU} \sim 10^{15} \text{ cm}$ (see Edwards *et al.* 1987; ALS), which is also consistent with the disk size expected from theories of star/disk formation (see, e.g., Cassen and Moosman 1981; Terebey, Shu, and Cassen 1984). Determination of the disk masses M_D for these systems requires (previously unavailable) data at submillimeter wavelengths, where the disk emission is likely to be optically thin. In this present work, we find that our submillimeter observations are consistent with the disk model outlined above; we then use our observations to estimate the disk masses for these systems.

At submillimeter wavelengths, essentially all the observed emission must originate in the circumstellar disk (or some other *nonstellar* component). Consider, for example, a “typical” T Tauri star with a radius $R_* \sim 1.5 \times 10^{11} \text{ cm}$, a luminosity $L_* \sim 5 L_\odot$, and a surface temperature $T_* \sim 4500 \text{ K}$ (see, e.g., the reviews of Cohen 1984 and Bertout 1989). At the distance (140 pc) of Taurus, our generic star will have a flux density of $\sim 3.8 \times 10^{-5} \text{ Jy}$ ($3.8 \times 10^{-6} \text{ Jy}$) at a wavelength of $\lambda = 350 \mu\text{m}$ (1100 μm). Thus, the expected stellar flux density is approximately five orders of magnitude smaller than the observed flux density at submillimeter wavelengths.

For the observations of this work, we chose stars which are suspected of having circumstellar disks. The sources T Tau,

¹ Harvard-Smithsonian Center for Astrophysics.² Physics Department, Queen Mary and Westfield College.³ Astronomy Department, University of California, Berkeley.

DG Tau, HL Tau, HK Tau, HP Tau, UY Aur, DK Tau, SR 9, and VSSG 23 were chosen for study because they all exhibit spectral energy distributions which are consistent with the presence of circumstellar disks and have been modeled previously (ALS; Adams, Lada, and Shu 1987). The sources HN Tau, DO Tau, FS Tau, and GM Aur were also observed. The first three of these objects were among those with the largest values of luminosity ratio L_{bol}/L_{\star} (2.34–4.26), which indicates the presence of circumstellar disks (CEB). HN Tau, DO Tau, and FS Tau are all O I stars, which provides further indication of disks (CEB). In addition, HN Tau and DO Tau show only blue-shifted O I emission, which suggests that an opaque disk is obscuring the redshifted emission (Edwards *et al.* 1987). The source FS Tau (also known as Haro 6–5) has *JHKL* colors similar to those of DG Tau and HL Tau, both of which are likely to have disks (see above); in addition, the polarization morphology of FS Tau also suggest that it has a disk (Gledhill and Scarrott 1989). Finally, the source GM Aur was observed because it has significant emission at *IRAS* wavelengths; however, GM Aur has a relatively low luminosity ratio $L_{\text{bol}}/L_{\star} = 1.04$ (CEB), which may be indicative of no significant disk.

The paper is organized as follows. We first describe the observational procedure (§ II) and then discuss the observational results (§ III). In the following section, § IV, we outline the theory of emission from star/disk systems (from ALS); we then compare our data with the theoretical model in § V and derive mass estimates for some of the sources. Finally, we discuss our results and conclusions in § VI.

II. OBSERVATIONS

a) Instrument and Method

The observations for this paper were performed using the common user He³ bolometer system UKT14 (see Duncan *et al.* 1989) at the Nasmyth focus of the 15 m James Clerk Maxwell Telescope⁴ (JCMT) on Mauna Kea, Hawaii. Most of the data were taken on 1989 January 23 (UT) with additional measurements on January 22, 24, and 25. The two objects in Ophiuchus (SR 9 and VSSG23) were measured on 1988 June 29 and 30 UT).

The data were taken in the usual chopping and beam switching mode with a chop throw of 120" in azimuth. Since the telescope pointing accuracy was not perfect (the pointing uncertainty was ~4"–5"), we choose the largest available aperture size (65 mm—see Table 1 for the corresponding FWHM [full width at half-maximum] beam size) to ensure that we included any extended emission (e.g., from a circumstellar disk). Since the expected disk size is $R_D \sim 100$ AU for these systems, the expected angular diameter is approximately 2" at the distance (140 pc) of the Taurus molecular cloud. Hence, the relatively large beam size (16"–19"—see Table 1) that we used should be adequate to collect most of the disk emission. In order to minimize pointing errors, we regularly peaked up on a nearby bright source of known position using a five point routine. For sources in Taurus, we used HL Tau for this purpose and then, having made any necessary pointing corrections, we moved to the nearby object of interest.

⁴ The James Clerk Maxwell Telescope is operated by the Royal Observatory Edinburgh on behalf of the Science and Engineering Research Council of the United Kingdom, the Netherlands Organisation for Scientific Research, and the National Research Council of Canada.

TABLE 1
SYSTEM CHARACTERISTICS

λ (μm)	ν_{eff} (GHz)	$\Delta\nu_{\text{eff}}$ (GHz)	FWHM ^a (arcsec)	\mathcal{E}^a (Jy/mV ⁻¹)
1100.....	272	74	18.4	12.4
800.....	380	101	15.8	8.9
600.....	463	112	17	12.4
450.....	676	84	18	16.3
350.....	854	113	19	25.2

^a For the 65 mm aperture.

Observations were made with bandpass filters at nominal wavelengths of 1100, 800, 600, 450, and 350 μm . The filters are designed to be matched to the appropriate atmospheric windows, but the effective frequency and band pass are dependent on the water vapor content of the atmosphere at the time of observation, particularly for the shorter wavelength windows. The effective frequency and bandwidth of each filter are given in Table 1 for 1 mm of precipitable water vapor.

b) Calibration Sources

Mars was used for most of our calibrations. During the observations, the angular semidiameter θ_P of Mars ranged from 3"98 to 3"89 (see Table 2) on the sky. For each night, the

TABLE 2A
ATMOSPHERE AND CALIBRATION DATA FOR TAURUS

λ (μm)	Transmission (%)	$\Delta\tau$	τ range	T_B Mars (K)	T_B Jupiter (K)
1989 Jan 22 ($\theta_{\text{Mars}} = 3''98$, $\theta_{\text{Jupiter}} = 20''95$)					
1100.....	75	0.05	0.4–0.2	203.6	170
800.....	40	0.1	1.1–0.5	202.7	162.5
600.....	10	0.2	2.5–1.5	202.1	...
1989 Jan 23 ($\theta_{\text{Mars}} = 3''95$, $\theta_{\text{Jupiter}} = 20''87$)					
1100.....	80	0.01	0.3–0.1	203.5	170
800.....	65	0.1	0.5–0.2	202.6	162.5
600.....	40	0.1	1.0–0.8	202.0	...
450.....	30	0.1	1.4–1.1	200.9	148.5
350.....	25	0.1	1.6–1.2	200.3	143.2
1989 Jan 24 ($\theta_{\text{Mars}} = 3''92$, $\theta_{\text{Jupiter}} = 20''81$)					
1100.....	70	0.05	0.45–0.30	203.4	170
1989 Jan 25 ($\theta_{\text{Mars}} = 3''89$, $\theta_{\text{Jupiter}} = 20''74$)					
1100.....	75	0.1	0.6–0.2	203.3	170
800.....	30	0.2	1.8–0.8	202.4	162.5

TABLE 2B
ATMOSPHERE AND CALIBRATION DATA FOR OPHIUCHUS

λ (μm)	Transmission (%)	$\Delta\tau$	τ range	T_B Uranus (K)
1988 Jun 29 ($\theta_{\text{Uranus}} = 1''93$)				
1100.....	75	0.05	0.4–0.2	92.5
800.....	50	0.1	0.9–0.7	83.7
1988 Jun 30 ($\theta_{\text{Uranus}} = 1''93$)				
1100.....	90	0.05	0.16–0.06	92.5
800.....	65	0.05	0.5–0.4	83.7
450.....	25	0.05	1.5–1.4	68.2

expected flux density from Mars was calculated at each wavelength using the planetary brightness temperature (predicted from the model of Wright 1976), the semidiameter of Mars, and a flux correction factor K . The flux factor K arises because not all the flux from a finite sized object will be weighted evenly by the (Gaussian) beam of the telescope. For a point source, the factor K would be unity; for Mars, K differed from unity by 6%–8%, depending on the wavelength. The assumption that the beam is Gaussian is likely to be incorrect for large angular radii due to the telescope sidelobe response, particularly at the shorter wavelengths. However, for an object like Mars which is compact compared to the beam size, the associated error is likely to be small.

Jupiter (which had a semidiameter of $20''.95$ – $20''.74$ —see Table 2) was used for additional calibrations. These calibrations are more likely to be affected by errors in the assumption of a Gaussian beam shape and by atmospheric variations with direction (since Jupiter and Taurus were in a different part of the sky). Fortunately, however, atmospheric extinctions derived from Mars and from Jupiter were in good agreement, which gives us confidence in our calibration method. The brightness temperature for Jupiter was taken from Griffin *et al.* (1986), which also gives a useful discussion of the Mars calibration model used here.

Uranus was used for all of our calibrations in Ophiuchus. During the observations, the angular semi-diameter of Uranus was $1''.93$ on the sky. For each night, the expected flux density from Uranus was calculated at each wavelength using the semidiameter of Uranus and the brightness temperature for Uranus (taken from Griffin *et al.* 1986 and Orton *et al.* 1986).

We estimate the overall systematic uncertainty in the calibration as 5%–10%. Most of this error arises from uncertainty in the adopted planetary brightness temperatures, which are given in Table 2. This systematic uncertainty is *not* included in any of our tabulations or discussion below; i.e., for the remainder of this paper, we will assume that the planetary brightness temperatures are correct. Keep in mind, however, that this systematic uncertainty is present in all of our results.

c) Atmospheric Extinction

The atmospheric transmission was not sufficiently stable to use plots of logarithm of signal strength against airmass to determine the extinction per unit airmass and the system response \mathcal{C} (Jy mV^{-1}) outside the atmosphere. Because the system response is known to be stable, we have adopted values for \mathcal{C} (see Table 1) and then used these to calculate the atmospheric extinction per unit airmass each time a calibration source was observed. The system response \mathcal{C} was determined by G. Sandell for a $90''$ chop using data from very stable nights and increased by 5% to account for our $120''$ chop (Sandell, private communication; JCMT internal report “Note to UKT14 users” 1988). When we could determine the system response, albeit with large uncertainties, the values were consistent with the adopted values which are based on many nights of good observing conditions which we cannot match.

The system response \mathcal{C} for $600 \mu\text{m}$ had not been measured previously and was determined directly from our data. The $600 \mu\text{m}$ filter response is very sensitive to the water vapor in the atmosphere and is thus very hard to calibrate (G. Sandell, private communication). The night of January 23 was sufficiently stable to determine the system response outside the atmosphere as 12.4 Jy mV^{-1} , at least for the conditions on that night. Even though this value may not be generally applicable,

we feel it is useful for our data for which the calibration and source observations are fairly closely matched in time and air mass. Because we have no other data, we also used this response for calibrating our $600 \mu\text{m}$ observation of HL Tau (taken on January 22), although the atmospheric transmission was 10%, a factor of 4 less than on January 23. We note that the resulting $600 \mu\text{m}$ flux densities fit smoothly onto the observed continuum spectra of the sources (see below); this result suggests that our $600 \mu\text{m}$ calibration must be approximately correct. However, we caution that our apparent success in calibrating $600 \mu\text{m}$ data may be solely due to the fortunate close relative location of the calibration source (Mars) and our objects.

The validity of the approach of assuming a system response is confirmed by noticing that, within the uncertainties, the deduced extinctions per unit air mass are the same using different calibration sources (Mars and Jupiter). Moreover, the trends found at different wavelengths correlate with one another as would be expected if the water vapor content of the atmosphere is changing with time (the atmosphere generally dries out during the night). The changes in transmission correlate credibly with changes in the humidity monitored at the telescope, and for $350 \mu\text{m}$ they were consistent with reports from $370 \mu\text{m}$ line observers on another telescope at the same time.

Tables 2A and 2B show the typical atmospheric transmission, the uncertainty in optical depth per unit air mass ($\Delta\tau$), and the range over which the optical depth per unit air mass varied for each night for the wavelengths used; also shown are the adopted brightness temperatures and angular semidiameters of Mars, Jupiter, and Uranus. Using our calibration data, we determined by interpolation the extinction per unit air mass at the time of the photometry on our sources; we then used this extinction in conjunction with the adopted system response (i.e., \mathcal{C}) to determine our flux densities.

III. RESULTS

a) Large Beam Photometry

Most of the observations for this paper were made on 1989 January 23. In addition, on January 22, we measured HL Tau at $1100, 800, 600 \mu\text{m}$; on January 24, we measured DO Tau, HK Tau, HL Tau, GM Aur, and the upper limits for DK Tau, HN Tau, and HP Tau, all at $1100 \mu\text{m}$; on January 25, we measured HL Tau and GM Aur at 1100 and $800 \mu\text{m}$, and UY Aur, HN Tau at $1100 \mu\text{m}$; on 1988 June 29, we measured VSSG23 at 1100 and $800 \mu\text{m}$; on 1988 June 30, we measured VSSG 23 at 800 and $450 \mu\text{m}$ and SR9 at $1100 \mu\text{m}$. The quality of each night can be judged from Table 2 above. Table 3 presents our flux measurements, together with their uncertainties (or 3σ upper limits), for the T Tauri systems we detected, and Table 4 presents our 3σ upper limits. The $800 \mu\text{m}$ upper limit ($<0.15 \text{ Jy}$) for FS Tau was obtained using a $13''.5$ beam (47.3 mm aperture).

We also detected “ZZ Tau FIR” at $1100 \mu\text{m}$ with a flux density $0.11 \pm 0.02 \text{ Jy}$ on 1989 January 24. This detection, and the *IRAS* photometry for this source, refer not to the optical star ZZ Tau but to the *IRAS* source 04278+2435 which lies $\sim 37''.5$ south of the optical star. Examination of co-added raw *IRAS* data at the optical star’s position and assessment of the *IRAS* pointing shows that the *IRAS* source is clearly *not* coincident with the optical star. In view of this finding, we do not consider this object any further in this present work and point

TABLE 3
MEASURED FLUX DENSITIES^a FOR T TAURI SYSTEMS

Source	$F_{\nu}(1100 \mu\text{m})$ (Jy)	$F_{\nu}(800 \mu\text{m})$ (Jy)	$F_{\nu}(600 \mu\text{m})$ (Jy)	$F_{\nu}(450 \mu\text{m})$ (Jy)	$F_{\nu}(350 \mu\text{m})$ (Jy)
T Tau	0.32 ± 0.03	1.07 ± 0.11	1.3 ± 0.2	2.6 ± 0.4	8.5 ± 1.0
DG Tau	0.44 ± 0.03	0.94 ± 0.10	1.4 ± 0.2	3.6 ± 0.4	9.6 ± 1.1
HL Tau	1.11 ± 0.02	2.58 ± 0.19	4.3 ± 0.9
HK Tau	0.11 ± 0.02	0.21 ± 0.03	...	1.7 ± 0.4	<4.5
DO Tau	0.18 ± 0.02	0.21 ± 0.02	0.5 ± 0.1	<1.0	...
GM Aur	0.38 ± 0.03
VSSG 23	<0.05	0.25 ± 0.04	...	<0.7	...

^a The upper limits shown in the table are 3σ .

out that disk models of this source (e.g., ALS) should be treated with caution because the near-infrared data and the *IRAS* data do not refer to the same object.

Where several observations of a source were taken (as in most cases), we report the weighted mean and uncertainty. The uncertainty quoted includes *both* the statistical uncertainty in the detection *and* the calibration errors due to uncertainty in determining the atmospheric extinction (1% at 1100 μm and 10% at the shorter wavelengths for 1989 January 23—see Table 2) but *not* any systematic errors due to the uncertainty (5%–10%) in planetary brightness temperatures. A weighted signal-to-noise ratio of at least 5 was required for a detection. In most cases, the extinction uncertainty is at least an equal source of error to the detection uncertainty.

The sources T, DG, HL, and DO Tau were also measured by WSD in a 65 mm aperture using the same equipment. Our respective flux densities are mutually consistent within the combined uncertainties for the 800 and 1100 μm results. At 450 and 350 μm , the comparison is not so straightforward, because WSD report results for a 47 mm beam, whereas we used a 65 mm beam; however, on the whole, our results are in reasonable agreement with those of WSD.

Figures 1–10 show plots of our data, together with other results from the literature. The figures show that our results appear reasonable and suggest that we have been sufficiently conservative in our calibration and assignment of uncertainties.

b) Extent of Objects

The expected disk size is $R_D \sim 100$ AU for the T Tauri disk systems (see, e.g., Edwards *et al.* 1987; ALS), so the expected angular diameter is approximately $2''$ at the assumed distance (140 pc) for the Taurus molecular cloud. Hence, the relatively large beam sizes ($16''$ – $19''$) that we used should be adequate to collect most of the disk emission.

TABLE 4
 3σ UPPER LIMITS FOR T TAURI SYSTEMS

Source	$F_{\nu}(1100 \mu\text{m})$ (Jy)	$F_{\nu}(800 \mu\text{m})$ (Jy)
HP Tau	<0.1	...
DK Tau	<0.1	...
UY Aur	<0.1	...
FS Tau	$<0.15^a$
HN Tau	<0.1	...
SR 9	<0.05	...

^a The 800 μm point for FS Tau was taken using the 47.3 mm aperture (i.e., a $13''.5$ beam).

However, WSD report extended emission (in terms of E-W \times N-S angular size) for T Tau ($11''.3 \times 10''.7$, “clearly resolved”), HL Tau ($7''.5 \times 7''.5$, “may be resolved”), and DG Tau ($5''$ – $10''$ in the E-W direction, “probably resolved”). Their observations were performed with a beam size of $15''.8$ for HL and T Tau and $13''.5$ for DG Tau. For a Gaussian source and beam, the true source size θ_S is related to the measured source size θ_M and the beam size θ_B through the relation

$$\theta_S = (\theta_M^2 - \theta_B^2)^{1/2},$$

so that a source must have a size of greater than $8''.5$ to produce an effect of greater than 10% on the measured source size (for an $18''.5$ beam). The reported extents of DG Tau, T Tau, and HL Tau would produce effects of 21%, 14%, and 10%, respectively. Because of pointing uncertainties and changes in atmospheric transmission, measurements with this accuracy are very difficult to make. Since theories of star formation (see Shu, Adams, and Lizano 1987; ALS) do not predict such large extents, we have examined our data carefully to try to extract any information on the angular extent of our sources.

Using the same five point mapping techniques as WSD, we were unable to resolve the source HL Tau at 1100 μm with an $18''.4$ beam or at 800 μm with a $13''.5$ beam, nor were we able to resolve T Tau at 800 μm with a $13''.5$ beam (which is smaller than that used by WSD). However, for DG Tau at 350 μm , we found that the ratio of flux density in the 21 mm aperture to that in the 65 mm aperture was smaller for DG Tau than for Mars; this finding would imply that DG Tau is more extended than Mars, although this difference was only marginally significant. It is intriguing that an additional report of extended emission has been made (Cohen, Harvey, and Schwartz 1985) for DG Tau at 95 μm . However, because of the relatively poor observing conditions at 350 μm , we do not have great faith in our indication of extent. In addition, because of uncertainties in our knowledge of the beam shapes at 350 μm , we are unable to convert our flux ratio into a source size.

Thus, our measurements of HL, T, and DG Tau do *not* show clear evidence for extended emission at submillimeter wavelengths. However, given that the measurements presented here were not made under perfect atmospheric conditions and were made using a fairly large beam size, these measurements were not ideal for such attempts. Because of the difficulties in this kind of work, new measurements designed specifically to determine source sizes should be made (under good observing conditions) to confirm our results and those of WSD.

If future observations reveal that the T Tauri stars are indeed extended at submillimeter wavelengths, spectral synthesis studies (such as ALS) must be lacking a component, which may be an extended remnant dust envelope. However, the exis-

tence of extent is uncertain, and we will ignore this issue for the remainder of this paper. We do emphasize the importance of determining accurate source sizes (or upper limits) in the future because such measurements will provide a crucial test on theories of star/disk formation.

IV. THEORY OF EMISSION FROM STAR/DISK SYSTEMS

If we interpret the submillimeter emission as arising from a circumstellar disk, we can derive useful information about the basic disk properties. For this purpose, we will use the theoretical model of emission from star/disk systems developed previously by ALS (see also Adams, Lada, and Shu 1987). Although the theoretical model is already described in detail in ALS, we will summarize the basic features below and then discuss the implications for our submillimeter observations. Although we adopt a particular theoretical model to compare with our observations, the most important derived parameter—the disk mass M_D —can be determined independently of the theory (see § VI) for an assumed dust opacity.

In the ALS model, the total flux from the system is divided into two components: the stellar flux and the disk flux. The star is assumed to have a luminosity L_* which is a fraction of the total bolometric luminosity L_{bol} of the entire star/disk system. The stellar spectrum is that of a blackbody with a surface temperature T_* , which is determined by the spectral classification. Since we are interested mainly in the submillimeter portion of the spectrum where the star does not contribute, the details of the *stellar* spectrum are unimportant.

In order to determine the radiant flux from the disk, the temperature profile and surface density profile of the disk must be specified. In principle, circumstellar disks can either be *active* or *passive*, i.e., they can have intrinsic luminosity L_D or merely intercept and reprocess stellar photons (see Adams, Lada, and Shu 1987; Kenyon and Hartmann 1987). We will explicitly consider spatially thin active disks which have appreciable intrinsic luminosity L_D in addition to the energy fL_* intercepted from the star (the factor f is the fraction of the stellar luminosity that is intercepted and reprocessed by the disk and has the value $f = \frac{1}{4}$ in the limit of a spatially thin but optically thick disk). Disk systems often have observed spectra that are much flatter than that of a classical Keplerian accretion disk (see Lynden-Bell and Pringle 1974); hence, the disk temperature distributions must be flatter than the “standard” law $T_D \sim \varpi^{-3/4}$. The ALS model assumes that the temperature distribution produced by the intrinsic luminosity of the disk is a simple power law in radius ϖ ,

$$T_D(\varpi) = T_{D*} \left(\frac{R_*}{\varpi} \right)^q, \quad (1)$$

where the temperature scale T_{D*} is determined by the intrinsic disk luminosity. As discussed by ALS and Kenyon and Hartmann (1987), the index q of the temperature profile determines the observed slope of the spectral energy distribution. For wavelengths longer than the peak of the stellar spectrum (a blackbody at T_*) and shorter than the peak of a blackbody at the minimum disk temperature, the spectral energy distribution will have approximately a power-law form

$$\nu F_\nu \propto \nu^\beta \quad \text{where} \quad \beta = 4 - 2/q.$$

At present, no *a priori* theoretical explanation exists for temperature profiles of the form of equation (1), and the index q is a free parameter of the theory (see, however, Lin and Pringle

1990 and Adams, Ruden, and Shu 1989 for recent work related to this issue). (However, we again stress that the results [e.g., estimates of disk mass M_D] obtained in this present work do not depend on the origin of the temperature profile. For example, if the temperature profile is produced by disk flaring and reprocessing of stellar photons rather than by an intrinsic energy source, our estimates of disk masses and radii remain unchanged.) Many of the sources that we present in this paper have relatively flat spectra (see, e.g., Fig. 1) and hence $q \approx \frac{1}{2}$ (see ALS). The disk is also heated by stellar photons; this effect is included in the model (see ALS) but provides a relatively unimportant contribution to the emission at submillimeter wavelengths for sources which have appreciable intrinsic luminosities.

This disk is assumed to be spatially thin (with scale height $H \ll \varpi$) and to have an isothermal *vertical* structure. The surface density distribution of the disk also has a power-law form,

$$\sigma(\varpi) = \sigma_* \left(\frac{R_*}{\varpi} \right)^p, \quad (2a)$$

where σ_* is determined by the total mass of the disk M_D and the index p :

$$\sigma_* = \frac{(2-p)M_D}{2\pi R_*^2 [(R_D/R_*)^{2-p} - 1]}. \quad (2b)$$

Since the spectra are insensitive to the value of p for the parameter range of interest (see Fig. 4 of ALS), we use the value $p = 7/4$, the result for a disk built up from the rotating infall solution of the *protostellar* theory (see Cassen and Moosman 1981). This use of $p = 7/4$ is justified because T Tauri disk systems are thought to be later stages of evolution of protostellar objects. Keep in mind, however, that none of our results depend on the parameter p , and we simply adopt a single representative value. Specifying the coefficient of the surface density profile is equivalent to specifying the mass of the disk M_D , which is left as a free parameter of the theory. Introducing a surface density distribution with a finite mass allows the disk to be partially optically thin (the optical depth through the disk in a direction *normal* to the disk surface is given by $\tau_\nu^D \equiv \kappa_\nu \sigma[\varpi]$, where κ_ν is the opacity). In the limit that the disk becomes optically thick at all wavelengths (i.e., $M_D \rightarrow \infty$), the outer boundary of the disk defines a minimum disk temperature and hence a “turnover” wavelength in the spectrum (see ALS). By fitting this turnover in the spectrum, ALS obtained *lower limits* to the disk radius R_D for many of the disk systems considered in this paper (see also § V below). The dependence of the theoretical model on the assumed disk radius R_D is shown in Figure 2 of ALS for the optically thick ($M_D \rightarrow \infty$) limit and in Figure 3 of ALS for the finite optical depth (and finite disk mass) case.

Once the disk temperature and density distributions have been specified, the spectral energy distribution of the disk is completely determined. For an observer at distance r and polar angle θ , the total radiative flux density F_ν^D of the disk is given by (see ALS)

$$4\pi r^2 F_\nu^D = 4g_*(\theta) \cos \theta \int_{R_*}^{R_D} \pi B_\nu [T_D(\varpi)] \times \{1 - \exp[-\tau_\nu^D(\varpi)/\cos \theta]\} 2\pi \varpi d\varpi, \quad (3)$$

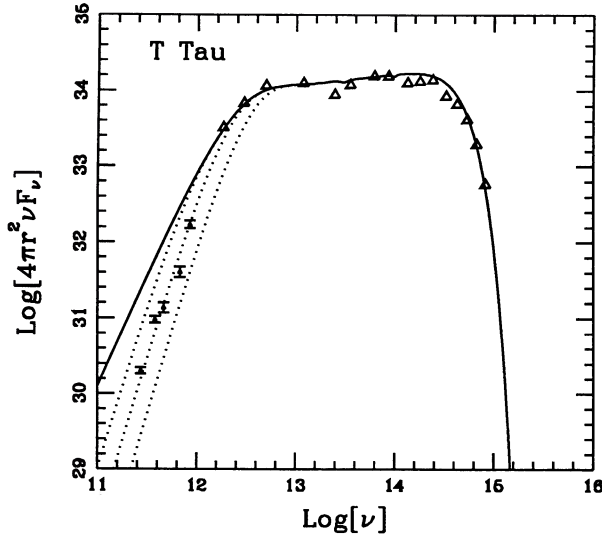


FIG. 1a

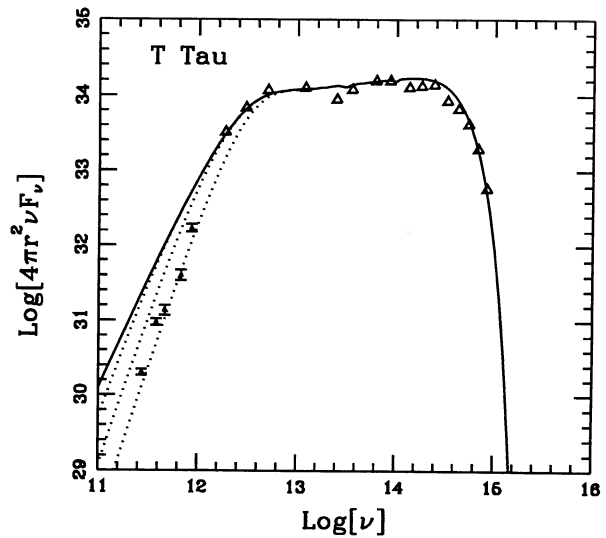


FIG. 1b

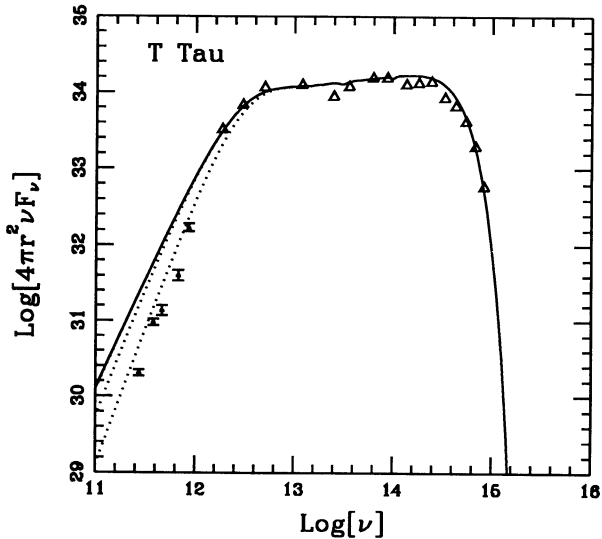


FIG. 1c

FIG. 1.—Spectral energy distribution of the infrared source T Tauri (cgs units). Open triangles are previously observed data points, solid triangles with error bars are the data points from this paper. Where no error bars are shown they are smaller than the plotting symbols. Solid curve shows the theoretical spectrum in the optically thick ($M_D \rightarrow \infty$) limit; dotted curves show spectra for finite disk masses of 0.01, 0.1, and $1.0 M_\odot$. (a) Models with “standard” opacity law $\kappa_\nu \sim \nu^2$ at low frequencies. (b) Models with alternate opacity law $\kappa_\nu \sim \nu^{3/2}$ at low frequencies. (c) Models with alternate opacity law $\kappa_\nu \sim \nu^1$ at low frequencies.

where R_D is the radius of the disk, B_ν is the Planck function, and $g_*(\theta)$ is the mean shadowing function (i.e., g_* accounts for occultation of the disk by the star—see the Appendix to ALS; see also Adams and Shu 1986). In general, the flux density will be attenuated by a factor $\exp(-\tau_\nu)$ due to extinction by interstellar material, i.e., material that is not associated with the source. However, the interstellar optical depth will be negligible at submillimeter wavelengths (typically the visual extinction $A_V = \mathcal{O}(1)$ so that $\tau_\nu \leq 10^{-4}$ for the observations of this paper). Notice also that the stellar temperatures and visual

extinctions are measured independently of the spectra (we adopt the values from Cohen and Kuhi 1979) and thus are *not* free parameters in the model.

V. COMPARISON OF THEORY AND OBSERVATIONS

In the following sections, we compare the complete (including submillimeter data) spectral energy distributions of T Tauri stars with the ALS theoretical models described above. To *leading order*, for a given temperature distribution, the disk emission at submillimeter wavelengths (see eq. [3]) is proportional to the disk mass,

$$F_\nu^D \propto \kappa_\nu M_D,$$

so that flux measurements can be used to estimate disk masses. Keep in mind, however, that the proportionality factor is a rather complicated function which depends on the disk surface density and temperature distributions. The disk mass estimates depend on the submillimeter opacity (κ_ν). We use the opacity profile of the ALS model, which assumes a mixture of graphite and silicate dust grains and produces a profile of the form $\kappa_\nu \propto \nu^2$ at low frequencies (long wavelengths); this opacity profile is consistent with that of Draine and Lee (1984) and has a value of $\kappa_\nu = 2.38 \times 10^{-3} \text{ cm}^2 \text{ g}^{-1}$ at a wavelength of $1100 \mu\text{m}$. It should be borne in mind that grains in accretion disks around T Tauri stars may be different from those considered by Draine and Lee (1984); for example, Wright (1987) suggests that fractal dust grains may have $\kappa_\nu \propto \nu^1$. Our calculated disk masses may be simply scaled if the reader prefers to adopt a different value of κ_ν . In order to compare theory and observations, we must also specify the distance to the sources; in the discussion that follows, we assume that the distance to the Taurus molecular cloud is 140 pc and that the distance to the Ophiuchus cloud is 160 pc.

Many stars are in binary systems, and several T Tauri stars have observed companions (e.g., Dyck, Simon, and Zuckerman 1982; Leinert and Hass 1989; Herbig and Bell 1988); however, we assume for simplicity that each observation refers to a single star/disk system, or that the effect of any companion on our results is negligible. Since we primarily interpret our data in terms of disk masses, even if we could include the effect of

possible companions, it seems unlikely that the resulting disk masses would change significantly.

a) T Tauri

We will first consider the eponymous young star T Tauri, whose complete spectral energy distribution is shown in Figures 1a, 1b, and 1c. The measurements of this paper are shown as solid triangles with error bars. Notice that because many T Tauri stars are variable and the observations are not simultaneous, the uncertainties in the plotted fluxes probably tend to underestimate the true uncertainty in the spectral shape (particularly at optical wavelengths). The previously observed data are shown as open triangles and were taken from Cohen and Schwartz (1976), Rydgren, Strom, and Strom (1976), Harvey, Thronson, and Gatley (1979), and from *IRAS*. The curves show theoretical spectral energy distributions (from ALS) in the limit $M_D \rightarrow \infty$ (solid curve) and for disk masses of 0.01, 0.1, and 1.0 M_\odot (dotted curves). The ALS fit to the spectral energy distribution of T Tau uses a visual extinction of 1.44 mag, a stellar temperature of 5105 K, a stellar luminosity of $5.1L_\odot$, an intrinsic disk luminosity of $11.9L_\odot$, a disk temperature index $q = 0.515$, and a disk radius of 120 AU, with the corresponding dust temperature at the outer disk radius being 36 K. This stellar luminosity is consistent with the observationally deduced value of $7.1L_\odot$ (CEB). Figure 1a shows the theoretical models for the opacity law which has the form $\kappa_\nu \sim \nu^2$ at low frequencies; Figures 1b and 1c show the effects of using alternate opacity laws which have the forms $\kappa_\nu \sim \nu^{3/2}$ and $\kappa_\nu \sim \nu^1$, respectively, at low frequencies. For the opacity law $\kappa_\nu \sim \nu^2$ (Fig. 1a), the submillimeter observations are in good agreement with the ALS disk model with $M_D = 0.1 M_\odot$; for the $\kappa_\nu \sim \nu^{3/2}$ opacity law, the disk mass estimate becomes $M_D \approx 0.02 M_\odot$; for a $\kappa_\nu \propto \nu^1$ opacity law, the disk mass estimate becomes $M_D \sim 0.002 M_\odot$.

Our interpretation of the submillimeter emission as arising from a disk is complicated by the presence of T Tauri's companion (see Dyck, Simon, and Zuckerman 1982). However, the total luminosity of the companion is likely to be much less than that of the disk (which has $L_D \sim 12L_\odot$). For example, one model of the companion (Dyck, Simon, and Zuckerman 1982) implies a luminosity of $1.5L_\odot$ and a surface temperature of 800 K. Not only is the total luminosity only about 10% of the disk luminosity, but the $1100 \mu\text{m}$ flux from such a star would only be $\sim 6 \times 10^{-4}$ Jy, which is three orders of magnitude smaller than the observed flux. In general, no starlike object (i.e., an object with a single temperature photosphere) can have an appreciable contribution to the submillimeter emission. Alternatively, it has been suggested (Bertout 1983) that the companion to T Tau is a protostar which could produce a significant contribution to the emission at *IRAS* and submillimeter wavelengths. CEB also discuss the possible contribution of the southerly companion to T Tau. Although the effect of a protostellar companion is difficult to assess, the presence of a luminous disk is consistent with the rather good agreement between theory and observation shown in Figure 1. In any case, in estimating a disk mass for this source, we assume that the companion does not contribute significantly to the observed submillimeter emission. However, high-spatial resolution submillimeter observations would be desirable to test this assumption.

Comparison of Figures 1a, 1b, and 1c shows that the present data cannot distinguish among dust emissivity indices n in the range 1–2, where the opacity $\kappa_\nu \propto \nu^n$. WSD attempted to derive

values of the indices n for T Tau and other T Tauri stars using their submillimeter observations. They assumed both optically thin emission and the Rayleigh-Jeans approximation (i.e., $h\nu/kT \ll 1$) and then deduced dust opacity index values which are too small to be physically plausible (see Emerson 1988 for an elementary review of the expected dust opacity index values n). WSD briefly mention that their result implies that simple isothermal and homogeneous models cannot explain the data. However, the disk temperature $T_D(R_D)$ at the outer disk radius predicted by the ALS models are such that even at $1100 \mu\text{m}$ the Rayleigh-Jeans approximation is not valid. The fact that the temperature and surface density (and hence optical depth) of the disk both vary with radius further complicates the picture. Given these difficulties in determining the dust opacity spectral index, we will use the $\kappa_\nu \propto \nu^2$ opacity law for the remainder of our comparisons. *Keep in mind, however, that our disk mass estimates are dependent upon our adopted opacity profile.* We discuss the validity of this assumed opacity, which can be viewed as illustrative rather than definitive, in § VI.

b) DG Tauri

Next we consider the star DG Tau, which has the spectral energy distribution shown in Figure 2. The measurements of this paper are shown as solid triangles with error bars. The optical and infrared data (shown as open triangles) are taken from Cohen and Schwartz (1976), Rydgren, Strom, and Strom (1976), and the *IRAS* point source catalog. The curves show theoretical spectral energy distributions (from ALS) in the limit $M_D \rightarrow \infty$ (solid curve) and for disk masses of 0.01, 0.1, and 1.0 M_\odot (dotted curves). The ALS fit to the spectral energy distribution of DG Tau uses a visual extinction of 3.0 mag, a stellar temperature of 5495 K (or alternatively 3500 K shown by the dashed line), a stellar luminosity of $0.61L_\odot$, an intrinsic disk luminosity of $5.49L_\odot$, a disk temperature index $q = 0.51$, and a disk radius of 75 AU, with the corresponding dust temperature

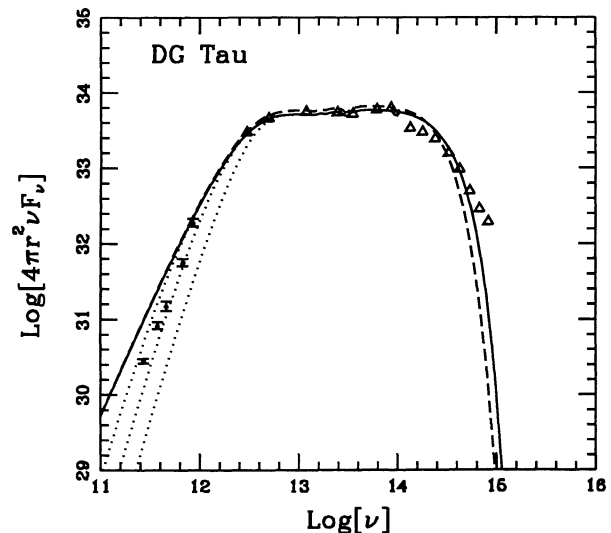


FIG. 2.—Spectral energy distribution of the infrared source DG Tauri (cgs units). Solid triangles are previously observed data points, solid triangles with error bars are the data points from this paper. Where no error bars are shown, they are smaller than the plotting symbols. Solid curve shows the theoretical spectrum in the optically thick ($M_D \rightarrow \infty$) limit for an assumed stellar photospheric temperature of 5495; the dashed curve assumes a cooler stellar surface temperature of 3500 K; dotted curves show spectra for finite disk masses of 0.01, 0.1, and 1.0 M_\odot .

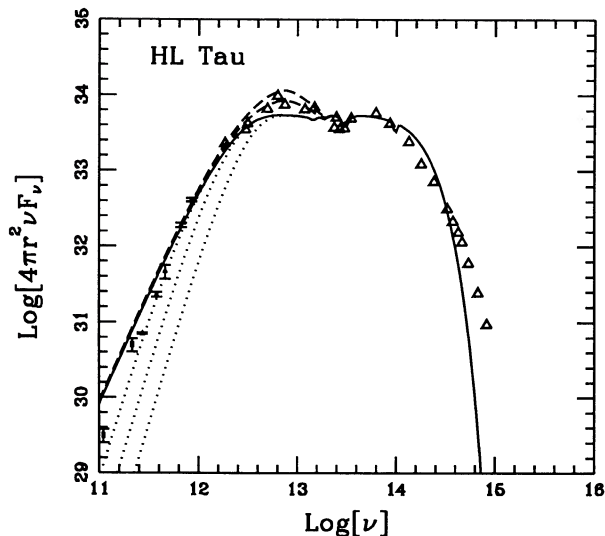


FIG. 3.—Spectral energy distribution of the infrared source HL Tauri (cgs units). Open triangles are previously observed data points; solid triangles with error bars are the data points from this paper, and solid squares with error bars are from WSD (at 350 and 450 μm) and from Woody *et al.* (1989) (at 1.4 and 2.7 mm). Where no error bars are shown, they are smaller than the plotting symbols. Solid curve shows the theoretical spectrum in the optically thick ($M_D \rightarrow \infty$) limit; dotted curves show spectra for finite disk masses of 0.01, 0.1, and 1.0 M_\odot . Dashed curves show the additional flux contribution of a residual infalling dust envelope surrounding the entire star/disk system for covering fractions of 0.5 and 1.0.

at the outer radius being 37 K. In this case, the submillimeter data imply a disk mass of between 0.1 and 1.0 M_\odot ; we crudely estimate the disk mass to be $M_D \approx 0.3 M_\odot$.

c) HL Tauri

Next we consider the star HL Tau, which has the spectral energy distribution shown in Figure 3. The measurements of this paper are shown as solid triangles with error bars; since we did not obtain measurements for this source at 350 and 450 μm , we have used the data of WSD at these wavelengths. We have also included the 2.7 and 1.4 mm data from Woody *et al.* (1989). The short-wavelength data ($\lambda \leq 10 \mu\text{m}$) come from the catalog of Rydgren *et al.* (1984), which in turn is a compendium from Cohen and Schwartz (1976), Rydgren, Strom, and Strom (1976), Rydgren and Vrba (1981, 1983), Strom, Strom, and Vrba (1976), and Cohen (1980). For $\lambda \geq 20 \mu\text{m}$, the data are from Cohen (1983), the *IRAS* point source catalog, and from CEB at 100 μm . Since the *IRAS* beam includes both HL Tau and XZ Tau, the measured flux must be divided between the two sources; this is done under the assumption that each source contributes a constant fraction of the total flux, with the fraction determined by the ratio of the resolvable fluxes from the sources (CEB). This separation of fluxes was *not* performed for the submillimeter data shown in Figure 3, because the submillimeter beam was small enough to exclude XZ Tau.

The curves show theoretical spectral energy distributions (from ALS) in the limit $M_D \rightarrow \infty$ (solid curve) and for disk masses of 0.01, 0.1, and 1.0 M_\odot (dotted curves). The ALS fit to the spectral energy distribution of HL Tau uses a visual extinction of 7.0 mag, a stellar temperature of 4000 K, a stellar luminosity of $1.0L_\odot$, an intrinsic disk luminosity of $5.0L_\odot$, a disk temperature index $q = 0.501$, and a disk radius of 100 AU,

with the corresponding dust temperature at the outer radius being 34 K.

In this case, the submillimeter data imply a rather large disk mass of approximately 1.0 M_\odot . In the far-infrared, the source exhibits excess emission which cannot be accounted for by a simple star/disk system. The ALS model shown in Figure 3 invokes a residual infalling dust envelope to describe this effect (see the dashed curves). However, the estimated mass in the infalling shell is small compared to our disk mass estimate of 1.0 M_\odot . The total mass is the infalling shell is estimated to be approximately $10^{-4} M_\odot$ from observed scattered emission (Beckwith *et al.* 1984; Grasdalen *et al.* 1984). Hence, the estimate of the disk mass obtained from submillimeter observations should not be seriously affected by the presence of the dust shell.

d) HP Tauri

Next we consider HP Tau, which has the spectral energy distribution shown in Figure 4. The 1100 μm upper limit is from this paper, and the 800 and 450 μm flux densities are from WSD. The shorter wavelength data are from *IRAS* and Rydgren and Vrba (1983). The curves show the theoretical spectral energy distributions (from ALS) in the limit $M_D \rightarrow \infty$ (solid curve) and for disk masses of 0.01, 0.1, and 1.0 M_\odot (dotted curves). The ALS fit to the spectral energy distribution of HP Tau uses a visual extinction of 2.32 mag, a stellar temperature of 4775 K, a stellar luminosity of $1.26L_\odot$, a disk temperature index $q = 0.533$, and a disk radius of 100 AU, with the corresponding dust temperature at the outer radius being 20 K. As shown in Figure 4, the submillimeter data imply a disk mass somewhere between 0.01 and 0.1 M_\odot , and we estimate a best fit of approximately 0.05 M_\odot . However, for this source, it has been suggested that only about half the *IRAS* flux density can be attributed to HP Tau itself (see CEB); the remaining emission originates from

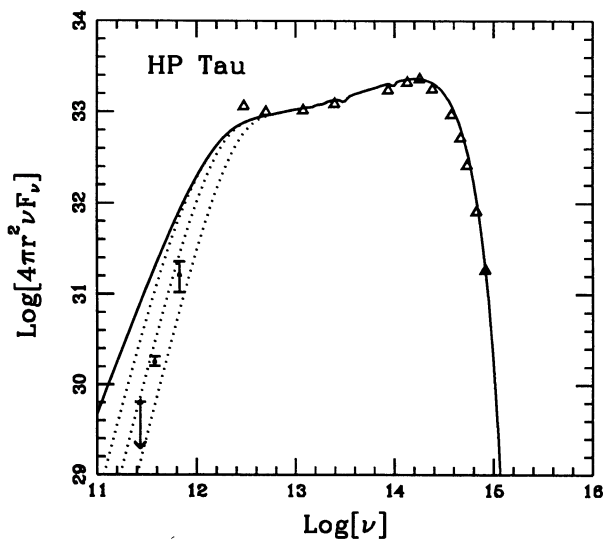


FIG. 4.—Spectral energy distribution of the infrared source HP Tauri (cgs units). Open triangles are previously observed data points, and solid triangles with error bars are the data points from this paper (at 1100 μm) and from WSD (at 800 and 450 μm). Where no error bars are shown, they are smaller than the plotting symbols. Solid curve shows the theoretical spectrum in the optically thick ($M_D \rightarrow \infty$) limit; dotted curves show spectra for finite disk masses of 0.01, 0.1, and 1.0 M_\odot .

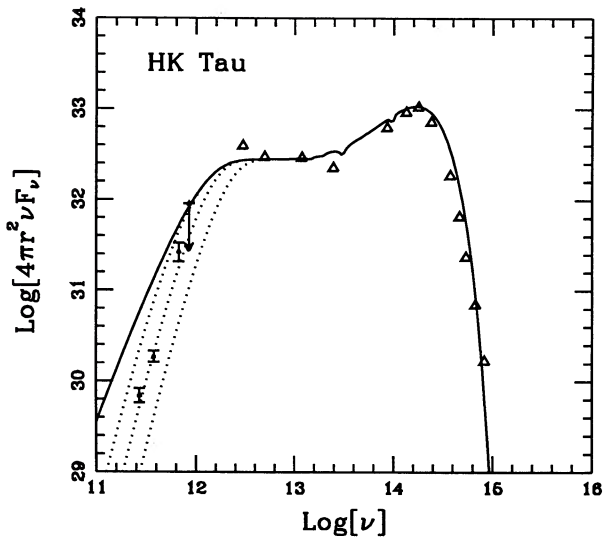


FIG. 5.—Spectral energy distribution of the infrared source HK Tauri (cgs units). Open triangles are previously observed data points, and solid triangles with error bars are the data points from this paper. Where no error bars are shown they are smaller than the plotting symbols. Solid curve shows the theoretical spectrum in the optically thick ($M_D \rightarrow \infty$) limit; dotted curves show spectra for finite disk masses of 0.01, 0.1, and $1.0 M_\odot$.

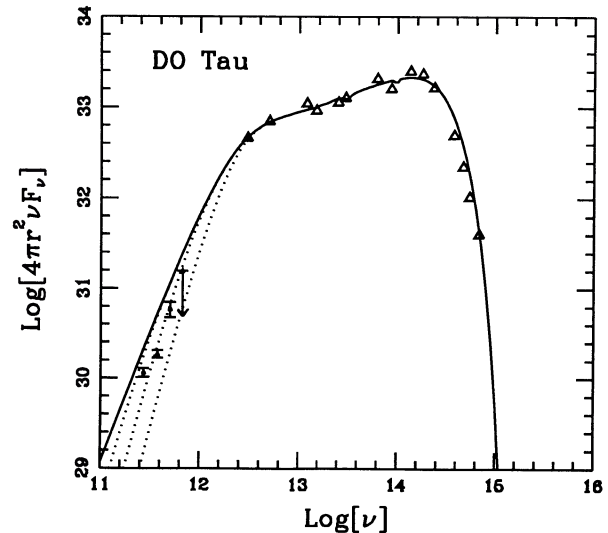


FIG. 6.—Spectral energy distribution of the infrared source DO Tauri (cgs units). Open triangles are previously observed data points, and solid triangles with error bars are the data points from this paper. Where no error bars are shown, they are smaller than the plotting symbols. Solid curve shows the theoretical spectrum in the optically thick ($M_D \rightarrow \infty$) limit; dotted curves show spectra for finite disk masses of 0.01, 0.1, and $1.0 M_\odot$.

HP Tau/G2 and HP Tau/G3. In this case, the theoretical model needs modification, and the disk mass estimate will be reduced. Unfortunately, HP Tau and HP Tau/G3 lie only $16''5$ apart and we cannot confirm the suggestion of CEB with the beam sizes used here.

e) HK Tauri

Next, we consider the HK Tau star/disk system, whose spectral energy distribution is shown in Figure 5. The measurements of this paper are shown as solid triangles with error bars. The shortwavelength data are taken from Rydgren, Schmeltz, and Vrba (1982), Rydgren and Vrba (1983), and from *IRAS*. The curves show theoretical spectral energy distributions (from ALS) in the limit $M_D \rightarrow \infty$ (solid curve) and for disk masses of 0.01, 0.1, and $1.0 M_\odot$ (dotted curves). The ALS fit to the spectral energy distribution of HK Tau uses a visual extinction of 3.42 mag, a stellar temperature of 3800 K, a stellar luminosity of $0.75L_\odot$, an intrinsic disk luminosity of $0.25L_\odot$, a disk temperature index $q = 0.501$, and a disk radius of 100 AU, with the corresponding dust temperature at the outer radius being 16 K. As shown in Figure 5, the submillimeter observations imply a disk mass in the range 0.1– $0.2 M_\odot$.

Notice that our mass estimate for HK Tau is the same as that for T Tau, even though the observed fluxes for T Tau are much larger (see Table 3). In order to fit the spectral energy distributions (see Figs. 1 and 5), the intrinsic disk luminosity of T Tau must be much greater than that of HK Tau; i.e., the disk of T Tau must be much hotter. Hence, the submillimeter emission (see eq. [3]) for T Tau can be correspondingly greater even though the masses are nearly the same. Another possibility exists: The viewing angle for the HK Tau system could be nearly $\pi/2$, i.e., nearly edge-on. If this were the case, the true disk luminosity would be higher than the apparent disk luminosity used here (see the discussion of ALS); hence, the disk mass would be overestimated using the procedure of this paper.

f) DO Tauri

Next we consider DO Tau, which has the spectral energy distribution shown in Figure 6. The measurements of this paper (at 1100, 800, 600, and $450 \mu\text{m}$) are shown as small solid triangles with error bars. The shorter wavelength data are from *IRAS* and Myers *et al.* (1987). DO Tau is a strong O I line star and has spectral type K7-M0 and hence a surface temperature of $T_* = 3960$ K (the same type as HL Tau, UY Aur, DK Tau, and GM Aur, which are also discussed in this work). The star lies on the $1 M_\odot$ convective sequence (CEB) and has a visual extinction of 1.35 ± 0.70 mag (Cohen and Kuhi 1979). CEB estimate the stellar luminosity to be $0.79L_\odot$ on observationally based grounds. For this source, Edwards *et al.* (1987) have estimated a disk radius of 69 AU based on the electron densities and emission measures of the optical [S II] lines and the failure to observe any redshifted lines. The curves show the theoretical spectral energy distribution in the limit $M_D \rightarrow \infty$ (solid curve) and for disk masses of 0.01, 0.1, and $1.0 M_\odot$ (dotted curves) for an ALS model (the source DO Tau was not considered by ALS). This fit to the spectral energy distribution uses a visual extinction of 2.05 mag (which is consistent with the estimate of Cohen and Kuhi 1979), a stellar temperature of 3960 K, a stellar luminosity of $0.5L_\odot$, an intrinsic disk luminosity of $1.2L_\odot$, a disk temperature index $q = 0.55$, and a disk radius of 40 AU, with the corresponding dust temperature at the outer radius being 30 K. The model implies a disk mass estimate of $0.1 M_\odot$.

g) GM Aurigae

GM Aur has the spectral energy distribution shown in Figure 7. The $1100 \mu\text{m}$ point is from this paper, the 800 and $450 \mu\text{m}$ flux densities are from WSD, the 100, 60, and $25 \mu\text{m}$ points are from *IRAS*, and the $12 \mu\text{m}$ point is from CEB. The shorter wavelength data are from Cohen and Kuhi (1979) and Rydgren and Vrba (1983). GM Aur does not have O I emission, and it has spectral type K7-M0 and hence $T_* = 3960$ K.

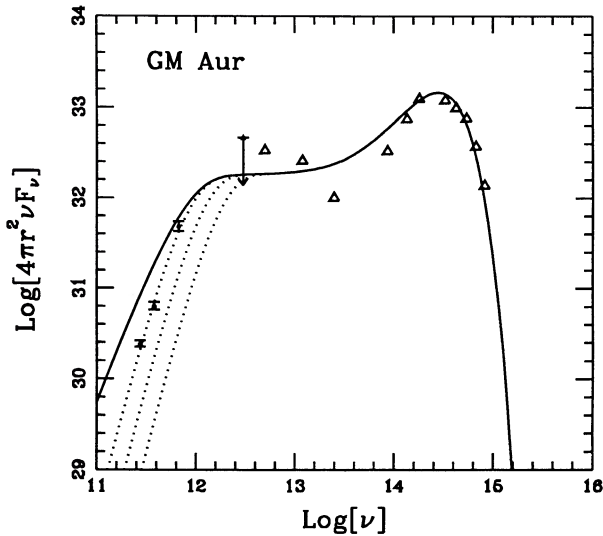


FIG. 7.—Spectral energy distribution of the infrared source GM Aurigae (cgs units). Open triangles are previously observed data points, and solid triangles with error bars are the data points from this paper (at $1100 \mu\text{m}$) and from WSD (at 800 and $450 \mu\text{m}$). Where no error bars are shown, they are smaller than the plotting symbols. Solid curve shows the theoretical spectrum in the optically thick ($M_D \rightarrow \infty$) limit; dotted curves show spectra for finite disk masses of 0.01 , 0.1 , and $1.0 M_\odot$.

The star lies on the $1 M_\odot$ convective sequence (CEB) and has a visual extinction of 0.14 mag. CEB estimate the stellar luminosity to be $1.13L_\odot$.

The observed spectrum of GM Aur shows a trace of “double-humped” structure (see Fig. 7) and does not fit the ALS model as well as the sources discussed above. The “extra” emission at far-infrared wavelengths *could* be due to source confusion in the *IRAS* beam, but the *IRAS* and optical positions for this source agree to within $7''$. However, the $100 \mu\text{m}$ point is an upper limit and, if the $12 \mu\text{m}$ point is ignored, the source can be fit with a flat-spectrum ALS model as shown. The curves show the theoretical spectral energy distributions in the limit $M_D \rightarrow \infty$ (solid curve) and for disk masses of 0.01 , 0.1 , and $1.0 M_\odot$ (dotted curves). This fit to the spectral energy distribution uses a visual extinction of 0.14 mag (which is consistent with the estimate of Cohen and Kuhl 1979), a stellar temperature of 3960 K, a stellar luminosity of $0.525L_\odot$, an intrinsic disk luminosity of $0.175L_\odot$, a disk temperature index $q = 0.502$, and a disk radius of 150 AU, with the corresponding dust temperature at the outer radius being 12 K. The model implies a disk mass estimate of nearly $1.0 M_\odot$; however, since this disk model does not provide a good fit to the mid-infrared data, the mass estimate should be regarded as tentative.

h) DK Tauri and UY Aurigae

DK Tau and UY Aur were two of the seven K7 T Tauri stars used by ALS to illustrate the spectra of more typical T Tauri stars. (The sources T, DG, HL, HP, and HK Tau are among the most extreme T Tauri stars.) For the source UY Aur, Edwards *et al.* (1987) have estimated a minimum disk radius of 64 AU, which is typical of the disks considered in this work. Since we only have upper limits of less than 0.1 Jy at $1100 \mu\text{m}$ for these two stars, we do not show the full spectral energy distributions for these sources.

The ALS fit to the composite spectrum used a stellar temperature of 4000 K, a stellar luminosity of $0.5L_\odot$, an intrinsic disk luminosity of $1.0L_\odot$, a disk temperature index $q = 0.6$, and a disk radius of 100 AU with the corresponding temperature at the outer disk edge being 12 K. We have computed a series of models with the same parameters and a range of disk masses. We crudely estimate that the observed $1100 \mu\text{m}$ upper limits require the disk masses to be $M_D < 0.1 M_\odot$ for both DK Tau and UY Aur.

i) FS Tauri/Haro 6-5a

Next we consider FS Tau, also known as Haro 6-5a, which has the spectral energy distribution shown in Figure 8. The $800 \mu\text{m}$ upper limit is from this paper, the 47 and $95 \mu\text{m}$ points are from Cohen, Harvey, and Schwartz (1985), the 60 , 25 , and $12 \mu\text{m}$ points are from *IRAS*, and the data at shorter wavelengths are from Vrba, Rydgren, and Zak (1985). Notice that the *IRAS* points and the 47 and $95 \mu\text{m}$ points seem to disagree; this discrepancy may be due to either extended emission or multiple sources in the *IRAS* beam (which is much larger than the KAO beam used by Cohen, Harvey, and Schwartz 1985). This interpretation is further supported by the finding that optical images of FS Tau show a lot of reflection nebulosity and structure (Gledhill and Scarrott 1989). In any case, our interpretation of FS Tau in terms of a theoretical star/disk model, which we present below, must be regarded as tentative. Although Haro 6-5b, which is associated with a Herbig-Haro object, also lies within the *IRAS* beam, it is 3.5 mag fainter (Vrba, Rydgren, and Zak 1985) than FS Tau at $3.4 \mu\text{m}$, so we ignore its effect here. FS Tau is a strong O I line star with spectral type M1 ($T_* = 3680$ K) and a visual extinction of 1.9 ± 0.3 mag (Cohen and Kuhl 1979); its short-wavelength colors are similar to those of DG Tau (Vrba, Rydgren, and Zak 1985) and there is evidence for a disk from polarimetry (Gledhill and Scarrott 1989).

In Figure 8, the curves show the theoretical spectral energy distributions in the limit $M_D \rightarrow \infty$ (solid curve) and for disk

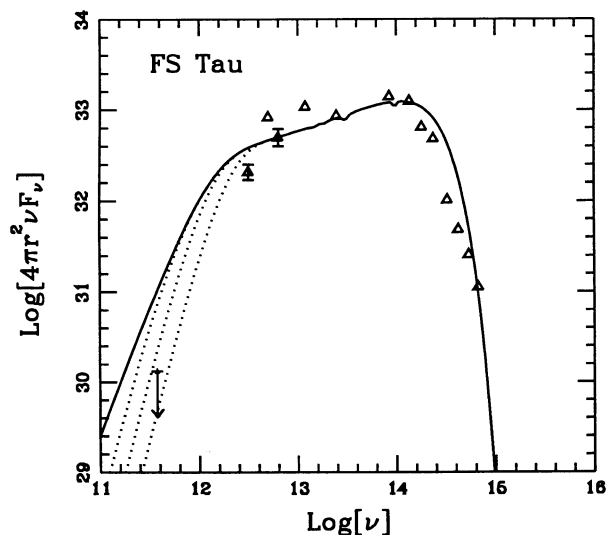


FIG. 8.—Spectral energy distribution of the infrared source FS Tauri (cgs units). Open triangles are previously observed data points, and the upper limit at $800 \mu\text{m}$ is from this paper. Where no error bars are shown, they are smaller than the plotting symbols. Solid curve shows the theoretical spectrum in the optically thick ($M_D \rightarrow \infty$) limit; dotted curves show spectra for finite disk masses of 0.01 , 0.1 , and $1.0 M_\odot$.

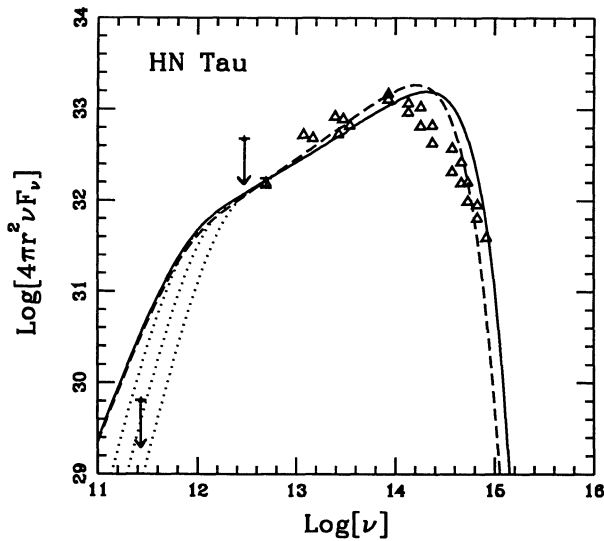


FIG. 9.—Spectral energy distribution of the infrared source HN Tauri (cgs units). Open triangles are previously observed data points, and upper limit at $1100 \mu\text{m}$ is from this paper. Where no error bars are shown, they are smaller than the plotting symbols. Solid curve shows the theoretical spectrum in the optically thick ($M_D \rightarrow \infty$) limit; dotted curves show spectra for finite disk masses of $0.01, 0.1,$ and $1.0 M_\odot$.

masses of $0.01, 0.1,$ and $1.0 M_\odot$ (dotted curves). The model uses a visual extinction of 2.5 mag (which is consistent with the estimate of Cohen and Kuhi 1979 at the 2σ level), a stellar temperature of 3680 K , a stellar luminosity of $0.15 L_\odot$, an intrinsic disk luminosity of $0.85 L_\odot$, a disk temperature index $q = 0.55$, and a disk radius of 75 AU , with corresponding dust temperature at the outer radius being 19 K . Because we only have an upper limit to the $800 \mu\text{m}$ flux density, we can only set an upper limit to the disk mass of $M_D < 0.08 M_\odot$.

j) HN Tauri

Next we consider HN Tau, which has the spectral energy distribution shown in Figure 9. The $1100 \mu\text{m}$ upper limit is from this paper, the $100 \mu\text{m}$ upper limit and the $60, 25,$ and $12 \mu\text{m}$ points are from *IRAS*, and the data at shorter wavelengths are from Rydgren *et al.* (1984), Rydgren, Strom, and Strom (1976), and from Rydgren, Schmeltz, and Vrba (1982). HN Tau is a strong O I line star with spectral type K5 ($T_* = 4395 \text{ K}$) and a visual extinction of $0.54 \pm 0.19 \text{ mag}$ (Cohen and Kuhi 1979). Both CEB and Strom *et al.* (1988) have argued that this object contains an active disk on the basis of its large ratio of bolometric to stellar luminosity, and Edwards *et al.* (1987) have estimated a disk radius of 65 AU based on the electron densities and emission measures of the optical [S II] lines and the failure to find any redshifted lines.

The curves show the theoretical spectral energy distributions in the limit $M_D \rightarrow \infty$ (solid curve) and for disk masses of $0.01, 0.1,$ and $1.0 M_\odot$ (dotted curves). The model uses a visual extinction of 0.73 mag (consistent with Cohen and Kuhi 1979), a stellar temperature of 4395 K , a stellar luminosity of $0.23 L_\odot$, an intrinsic disk luminosity of $0.67 L_\odot$, a disk temperature index $q = 0.6$, and a disk radius of 100 AU , with the corresponding dust temperature at the outer radius being 10.4 K . Notice that the observed data and the theoretical model do not agree very well in the $0.4\text{--}3.5 \mu\text{m}$ portion of the spectrum (i.e., $15.0\text{--}14.2$ in $\log \nu$). As illustrated by the dashed line in Figure 9,

this discrepancy can be reduced, but not eliminated, by using an M6 spectral type ($T_* = 3000 \text{ K}$) instead of the K5 spectral type found by Cohen and Kuhi (1979). This same discrepancy causes both CEB and Strom *et al.* (1988) to derive large values of L_{bol}/L_* . Thus, it would be of interest to have a confirmation of the spectral type of HN Tau. Because we only have an upper limit to the $1100 \mu\text{m}$ flux density, we can only set an upper limit to the disk mass of $M_D < 0.2 M_\odot$.

k) SR 9

We now come to two objects in Ophiuchus, for which we adopt a distance of 160 pc . The first source is SR 9, a K7 T Tauri star in Ophiuchus. Here, we only have an $1100 \mu\text{m}$ upper limit for this star, and we do not show its spectrum. The spectral energy distribution of SR 9 has been modeled (Adams, Lada, and Shu 1987) as a T Tauri star with a passive disk (i.e., with zero intrinsic disk luminosity); the model uses a visual extinction of 1.0 mag , a stellar temperature of 4000 K , and a stellar luminosity of $3.0 L_\odot$. We recomputed the model of Adams, Lada, and Shu (1987) using a range of disk masses and find that our 3σ upper limit to the $1100 \mu\text{m}$ flux density is consistent with the model but not sensitive enough to constrain the disk mass.

l) VSSG 23

The second object we consider in Ophiuchus is VSSG 23, whose “double-humped” spectral energy distribution is shown in Figure 10. The 1100 and $450 \mu\text{m}$ upper limits and the $800 \mu\text{m}$ detection are from this paper, the $100 \mu\text{m}$ upper limit and the $60, 25,$ and $12 \mu\text{m}$ points are from *IRAS*, and the data at shorter wavelengths are from Chini (1981) and Wilking and Lada (1983).

The source VSSG 23 has been modeled (Adams, Lada, and Shu 1987) as a T Tauri star with a passive disk and a residual circumstellar dust envelope. The model shown in Figure 10 uses a visual extinction of 5.0 mag , a stellar temperature of

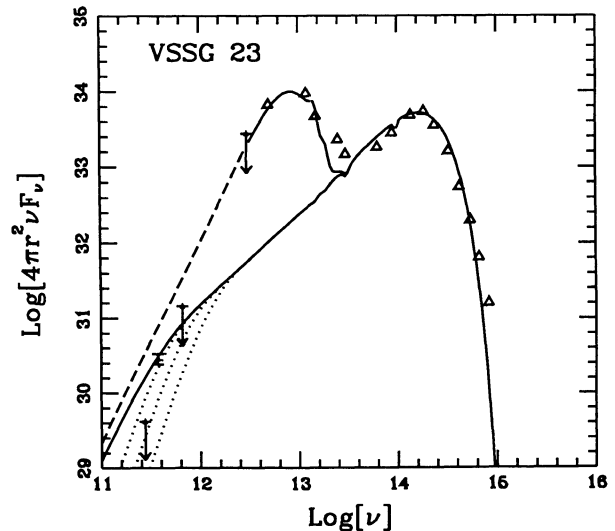


FIG. 10.—Spectral energy distribution of the infrared source VSSG 23 (cgs units). Open triangles are previously observed data points, and solid triangles with error bars are detections from this paper (at $800 \mu\text{m}$) and upper limits (at 1100 and $450 \mu\text{m}$). Where no error bars are shown, they are smaller than the plotting symbols. Solid curve shows the theoretical spectrum in the optically thick ($M_D \rightarrow \infty$) limit; dotted curves show spectra for finite disk masses of $0.01, 0.1,$ and $1.0 M_\odot$.

4500 K, a stellar luminosity of $6.0L_{\odot}$, and a disk radius of 100 AU, with the corresponding dust temperature at the outer radius being 6 K. The solid lines show the spectrum of the star/disk system in the limit $M_D \rightarrow \infty$ both with and without the dust envelope; for long wavelengths, $\lambda \geq 100 \mu\text{m}$, the simple model of the dust envelope (see Adams, Lada, and Shu 1987 for further details) overestimates the flux observed in a *finite* beam (the dust envelope extends out to spatial infinity), and the spectrum is shown as a dashed curve. The dotted curves show the theoretical spectra for finite disk masses of 0.01, 0.1, and $1.0 M_{\odot}$; thus, our 3σ upper limits and the $800 \mu\text{m}$ flux density suggest a disk mass of $\sim 0.2 M_{\odot}$, although this number is not very secure (see Fig. 10).

VI. DISCUSSION

The results of this work show that the spectral energy distributions of T Tauri star/disk systems are consistent with theoretical models of disk emission (e.g., ALS) and that the disk masses in these systems are in the range $0.05 M_{\odot} \leq M_D \leq 1.0 M_{\odot}$ for the assumed dust opacity. We also find that the disk radii are typically ~ 100 AU in these systems. These results are summarized in Table 5. Although the evidence for circumstellar disks is quite robust, the disk properties are not completely well determined. The estimates of the disk luminosity L_D depend on the amount of disk flaring, which determines the exact amount of the stellar luminosity which is reprocessed in the disk. Models of spectral energy distributions constrain the temperature profiles of the disks but do *not* determine the origin of the temperature profiles (see ALS and Kenyon and Hartmann 1987 for further discussion of this issue). The estimates of the disk mass M_D depend on the dust opacity at submillimeter wavelengths; we will address this issue more fully in the following discussion.

Although the current data are consistent with the theoretical models, the data do not set meaningful limits on the spectral index n of the dust opacity (see § Va above Figs. 1a, 1b, and 1c). Notice that both the observed spectral slope and the theoretical spectral slope (at submillimeter wavelengths) are much shallower than that suggested by the naive low-frequency approximation:

$$\nu F_{\nu}^D \propto \nu \kappa_{\nu} B_{\nu} \propto \nu^{(3+n)}, \quad (4)$$

where $n = 2$ is the spectral index of the opacity adopted here. In order for the approximation (4) to be valid, the quantity

$x \equiv h\nu/kT$ must be small, i.e., $x \ll 1$. However, for submillimeter wavelengths in the range $1100 \mu\text{m} \geq \lambda \geq 350 \mu\text{m}$, the quantity xT will be in the range $13.1 \leq xT \leq 41.2$, so that x is of order unity for typical temperatures at the outer disk edge (e.g., the outer disk temperature for the ALS model of T Tauri shown in Fig. 1 is $T_D(R_D) \sim 36$ K). Thus, the approximation (4) will only be valid for $\lambda \geq 1100 \mu\text{m}$ and cannot be used in the present context.

One of the greatest uncertainties in estimating the masses for T Tauri disks is the uncertainty in the dust opacity at submillimeter wavelengths. Although the spectral slopes seem consistent with the use of $\kappa_{\nu} \propto \nu^n$ with $n = 2$, smaller dust spectral indices cannot be ruled out. For example, if the spectral index were $n = 3/2$ (or $n = 1$) instead, and if the absolute scale of the opacity remained the same at $20 \mu\text{m}$, the opacity at $1100 \mu\text{m}$ would be approximately a factor of 7.4 (or 55) greater and the corresponding mass estimates would be lower by these factors (see Figs. 1b and 1c and ALS).

For dust grains found around T Tauri stars, the appropriate value of n in the submillimeter region of the spectrum is unknown because such grains may be different from the grains that have been more often studied in the interstellar medium. In a review of observational evidence, Hildebrand (1983) deduced $n = 2$ beyond $250 \mu\text{m}$ for interstellar dust grains. Draine and Lee (1984) find a similar value from their modeling of graphite and "astronomical silicate" materials. However, Tielens and Allamandola (1987) pointed out that in amorphous layered materials, such as amorphous carbon and layer-lattice silicates, the material structure limits phonons to two dimensions and should lead to $n = 1$; indeed, some materials studied in the laboratory show this behavior. Wright (1987) considered fractal dust grains, which might be formed by aggregation of small spherical grains, and showed that $n = 1$ in the submillimeter might be expected. The Kramers-Kronig relations show that for any grain material, $n \gtrsim 1$ as λ tends to ∞ in order to be consistent with causality (Purcell 1969).

Using the 1.4 and 2.7 mm flux densities for a number of young stellar objects (including HL Tau, DG Tau, and L1551 IRS 5), Woody *et al.* (1989) deduce $n = 1.0 \pm 0.2$; on the other hand, Keene and Masson (1990) deduce $n = 1.5 \pm 0.7$ for L1551 IRS 5 from a more extensive set of long-wavelength data. However, observational deductions of the value of n will tend to be systematically smaller than the true values if the assumptions of Rayleigh-Jeans emission or complete optical thinness are not correct. For grains around T Tauri stars n may lie toward the lower end of the range $n = 1-2$, and further careful observations of a larger sample of objects are required to resolve this question. In any case, the dust has not yet settled on this issue, but the dust opacity law with $\kappa_{\nu} \propto \nu^2$ remains a viable model (see Draine 1989).

It is also possible that the dust opacity is *smaller* than we have assumed here. If significant dust agglomeration has occurred, the grain sizes could become larger than the photon wavelength and the net opacity could decrease; this change in opacity would result in larger mass estimates than those given above. However, if too much grain agglomeration had occurred, the opacity law would no longer have the power-law form $\kappa_{\nu} \sim \nu^n$. In light of these uncertainties and in order to remain consistent with ALS, we have chosen to estimate disk masses using opacity values from the law of the form $\kappa_{\nu} \propto \nu^2$; notice, however, that our disk mass estimates can easily be scaled to incorporate any alternate choice of opacity.

However, except for the uncertainty in the opacity discussed

TABLE 5
DISK MASS AND RADIUS ESTIMATES
FROM SPECTRAL MODELS

Source	T_{RD} (K)	R_D (AU)	M_D (M_{\odot})
T Tau	36	120	0.1
DG Tau	37	75	0.3
HL Tau	34	100	1.0
HP Tau	20	100	0.05
HK Tau	16	100	0.15
DO Tau	30	40	0.1
GM Aur	12	150	1.0
DK Tau	12	100	<0.1
UY Aur	12	100	<0.1
FS Tau	19	75	<0.08
HN Tau	10	100	<0.2
SR 9	< ∞
VSSG 23	6	100	0.2

above, the estimates for the disk masses are fairly robust. To illustrate this claim, we will estimate the disk masses using a much simpler procedure: At sufficiently long wavelengths, we will assume that the disk emission is optically thin (but we retain the full Planck function) so that equation (3) can be written

$$4\pi r^2 F_\nu^D = 4\kappa_\nu \int_{R_*}^{R_D} \pi B_\nu[T_D(\varpi)] \sigma(\varpi) 2\pi\varpi d\varpi, \quad (5)$$

where we have set the shadowing function $g_*(\theta)$ equal to unity. Since circumstellar disks are expected to have temperature distributions which decrease outward, the lowest temperature in the disk will be at the edge where $T_D(R_D) \equiv T_{RD}$. If we then notice that $B_\nu[T_D(\varpi)] \geq B_\nu(T_{RD})$ everywhere in the disk, the emitted disk flux obeys the relation

$$4\pi r^2 F_\nu^D \geq 4\pi B_\nu(T_{RD}) \kappa_\nu M_D, \quad (6)$$

where we have evaluated the surface density integral to obtain the total disk mass M_D . Thus, provided that the opacity κ_ν and outer disk temperature T_{RD} can be determined, measurements (or upper limits) of the emitted disk flux imply upper limits to the disk mass. If we limit our discussion to 1100 μm data (where the emission is mostly likely to be optically thin), the mass limit can be written in the form:

$$M_D \leq \frac{F_\nu^D}{J_\nu} \left[\exp(13.1K/T_{RD}) - 1 \right] 1.32 M_\odot, \quad (7)$$

where we have used an 1100 μm opacity of $\kappa_\nu = 2.38 \times 10^{-3} \text{ cm}^2 \text{ g}^{-1}$ (per gram of material, not per gram of dust) from the $\kappa_\nu \propto \nu^2$ profile of ALS and where we have assumed a distance of 140 pc (appropriate for Taurus) to the sources. The relation (7) approaches equality if the outer portions of the disk provide the dominant contribution to the disk emission, i.e., if the temperature and surface density distributions are not overly steep. Notice that the temperature T_{RD} can be deduced from the frequency at which the spectrum "turns over" using the fact that the peak in $\nu\kappa_\nu B_\nu$ is $1.24 \times 10^{11} \text{ Hz K}^{-1}$ for $\kappa_\nu \propto \nu^2$. These turnover frequencies and the corresponding temperatures are tabulated in Table 6. Thus, we can make model-independent estimates of T_{RD} and use equation (7) to make relatively clean estimates/limits for the disk masses.

TABLE 6

DISK TEMPERATURE, RADIUS, AND MASS LIMITS FROM SIMPLE MODEL

Source	Turnover (log νL_ν)	T_{RD} (K)	$R_D \cos^{1/2} \theta$ (AU)	M_D (limit) (M_\odot)
T Tau	12.7	40	<200	<0.2
DG Tau	12.8	51	<80	<0.2
HL Tau	12.6	32	<380	<0.7
HP Tau ^a	12.4	20	<990	<0.2 ^b
HK Tau	12.5	25	<230	<0.1
DO Tau	12.5	25	<360	<0.2
GM Aur	12.4	20	<820	<0.5
DK Tau	12.7	40	<30	<0.1
UY Aur	12.7	40	<65	<0.1
FS Tau	12.5	25	<390	<0.1 ^b
HN Tau	12.6	32	<60	<0.1
SR 9	12.0	8	< ∞	<0.4
VSSG 23	12.8	51	<85	<0.1 ^b

^a Using HP Tau flux density at 800 μm from WSD.

^b Using flux densities at 800 μm .

The disk mass estimates/limits determined by the above procedure are shown in Table 6 (compare with the estimates from § V shown in Table 5). The crude mass estimates of this section agree with those from the ALS model (see § V) within a factor of 2; hence, the details of the model are not crucial in estimating disk masses, or, alternatively, we claim that the deduced disk masses are fairly well determined. We emphasize that the above simple argument for the disk masses is *independent* of the ALS models and is also independent of the origin of the disk temperature profile (which is determined by intrinsic disk luminosity sources and by reprocessing of stellar photons). Another independent argument exists for disk masses of this size: If the disk luminosity is due to accretion, the accretion rates through the disk must be of order $10^{-7} M_\odot \text{ yr}^{-1}$ (see below; see also ALS; Bertout, Basri, and Bouvier 1988; Hartmann and Kenyon 1987). Since the expected lifetime of these systems is of order 10^6 yr (Strom *et al.* 1989), the required reservoir of mass must be at least $0.1 M_\odot$, a value consistent with our estimates given above.

We can also use our temperature estimates T_{RD} and the observed flux densities at 60 μm , together with the assumption that the disk is optically thick at 60 μm , to deduce upper limits to the disk radii (actually, $R_D \cos^{1/2} \theta$), which are also given in Table 6. The radii are rather more strongly dependent (than the mass estimates) on the assumed dust temperature, and these estimates should be interpreted with caution. For four of our objects (DO Tau, HN Tau, HL Tau, and UY Aur), our upper limits to the disk radii may be compared with the estimates of the disk radii made by Edwards *et al.* (1987) based on the electron densities and emission measures of the optical [S II] lines and the failure to find any redshifted lines, which is interpreted as indicating obscuration by a disk. In each case, our estimate and that of Edwards *et al.* (1987) are mutually consistent. Our estimates are also consistent with the lower limits of ALS; given the uncertainties in these crude estimates, this agreement is encouraging.

For a random viewing angle, the *observed* luminosity of a star/disk system will *not* be equal to the true intrinsic luminosity of the system (see the Appendix to ALS). The observed apparent luminosity is related to the intrinsic stellar and disk luminosities (L_* and L_D) through equation (A45) of ALS. Thus, in order to quantify the observed size of the system luminosity relative to the stellar luminosity, we use the ratio L_{bol}/L_* where $L_{\text{bol}} = L_D^{\text{obs}}(\theta) + L_*^{\text{obs}}(\theta)$ and where $L_* = L_*^{\text{obs}}(\theta)$. In Table 7 we compare the values of L_{bol}/L_* predicted from the ALS model (using $\theta = \pi/4$) with the values of L_{bol}/L_* deduced from observations by CEB (when available). Except for the source FS Tau, the stars rank in almost the same order in both predicted and

TABLE 7

OBSERVED AND PREDICTED LUMINOSITY RATIOS

Source	L_{bol}/L_* (from CEB)	L_{bol}/L_* (this paper)
HN Tau	4.3	5.7
DO Tau	3.2	5.1
T Tau	2.7	5.1
FS Tau	2.4	9.7
UY Aur	2.3	4.4
HP Tau	2.3	3.3
DK Tau	1.8	4.4
HK Tau	1.2	2.0
GM Aur	1.0	2.0

TABLE 8
SPECIFIC DISK LUMINOSITY AND
EFFECTIVE ACCRETION RATES

Source	L_D/M_D (L_\odot/M_\odot)	\dot{M} ($10^{-7} M_\odot \text{ yr}^{-1}$)
T Tau	120	31
HP Tau	25	3.3
DG Tau	18	14
DO Tau	12	3.1
FS Tau	> 11	2.2
UY Aur	> 10	2.6
DK Tau	> 10	2.6
HL Tau	5.0	13
HN Tau	> 3.3	1.7
HK Tau	1.7	0.65
GM Aur	0.2	0.45
SR 9	0.0	0.0
VSSG 23	0.0	0.0

deduced L_{bol}/L_* and the absolute values mostly agree within a factor of 2, although the predicted values typically exceed the deduced values of CEB by 30%–90%. In the case of FS Tau, the ratios are different by a factor of 4. This discrepancy suggests that the models may have somewhat overestimated the true disk luminosities relative to those of the stars.

In fitting the observations, the model determines both the true luminosity of the disk L_D and the disk mass M_D . The specific disk luminosity L_D/M_D (i.e., the disk luminosity per unit mass of disk) is tabulated in Table 8 in units of L_\odot/M_\odot ; an effective mass accretion rate \dot{M} through the disk is also given. The quantity \dot{M} is determined by assuming that disk material is steadily accretion onto a stellar object and releases a luminosity L_D given by

$$L_D = \frac{GM_* \dot{M}}{2R_*}.$$

If we take the stellar mass to be $0.5 M_\odot$ and the stellar radius to be $2R_\odot$ (these are representative values for our sample of stars), we obtain the values for \dot{M} given in Table 8. The sources in Table 8 are listed in order of specific luminosity. We note that eight of the nine objects with the highest specific disk luminosity are also O I line stars; this finding confirms the relationship between disk activity and the winds responsible for the O I emission (suggested by CEB). The sources show a very large range in specific disk luminosity; this range suggests

that either the degree of disk activity varies rapidly with time (e.g., episodic outbursts) or that the physical processes generating the luminosity in these disks are not simply related to the disk mass. Although the accretion clearly does not follow the usual “classical” form (the spectral slopes are not $\nu F_\nu \sim \nu^{4/3}$), the effective steady accretion rates are found to be a few $\times 10^{-7} M_\odot \text{ yr}^{-1}$, which implies disk lifetimes of order 10^6 yr (unless the disk material can somehow be replenished).

The disk mass estimates that we obtain have important implications for theories of star formation and planet formation. First of all, it is significant that the range of disk masses is bounded from below by the value for the “minimum mass” solar nebula, i.e., the mass of the Sun’s planetary system augmented to solar abundances. Theories of planet formation have assumed that planets form from disks with masses at least as large as the “minimum mass” nebula. Our disk observations (which are for solar-type stars) indicate that this assumption may indeed be correct.

In addition, many of our disk mass estimates are significantly larger (e.g., HL Tau) than that of a “minimum mass” nebula. This result may also have important implications. Theoretical calculations (Adams, Ruden, and Shu 1989) indicate that when the disk mass is comparable to the stellar mass, spiral modes with azimuthal wavenumber $m = 1$ will grow on the dynamical timescale of the outer disk edge (i.e., $\tau \sim 10^3$ – 10^4 yr). Since this time scale is much shorter than the evolutionary time scale of these systems ($\tau \sim 10^5$ – 10^6 yr), spiral instabilities of this type may provide the accretion mechanism in these disks. These instabilities may also play a role in the formation of binary companions and/or giant planets within the disk (Adams, Ruden, and Shu 1989). Since some of our derived disk masses are comparable to the stellar mass, this mechanism could be important in the evolution of disks around young stars.

We are grateful to D. Brock, I. Coulson, and W. Duncan for their assistance at the telescope. In addition, we would like to thank S. Kenyon, C. Lada, P. Myers, R. Padman, A. Russell, and F. Shu for useful discussions. We are grateful to J. Pringle and an anonymous referee for useful comments on the manuscript. G. A. F. and F. C. A. acknowledge support from a grant from the California Space Institute. G. A. F. thanks Raman Research Institute, Bangalore, India for their hospitality during the writing of this paper; G. A. F. was supported in part by NSF (USA)-TIFR (India) grant number INT-8715411.

REFERENCES

- Adams, F. C., Lada, C. J., and Shu, F. H. 1987, *Ap. J.*, **312**, 788.
 ———. 1988, *Ap. J.*, **326**, 865 (ALS).
 Adams, F. C., Ruden, S. P., and Shu, F. H. 1989, *Ap. J.*, **347**, 959.
 Adams, F. C., and Shu, F. H. 1986, *Ap. J.*, **308**, 836.
 Beckwith, S., Sargent, A. I., Chini, R. S., and Gusten, R. 1990, preprint.
 Beckwith, S., Sargent, A. I., Scoville, N. Z., Masson, C. R., Zuckerman, B., and Phillips, T. G. 1986, *Ap. J.*, **309**, 755.
 Beckwith, S., Zuckerman, B., Skrutskie, M. F., and Dyck, H. M. 1984, *Ap. J.*, **287**, 793.
 Bertout, C. 1983, *Astr. Ap.*, **126**, L1.
 ———. 1989, *Ann. Rev. Astr. Ap.*, **27**, 351.
 Bertout, C., Basri, G., and Bouvier, J. 1988, *Ap. J.*, **330**, 350.
 Cassen, P., and Moosman, A., 1981, *Icarus*, **48**, 353.
 Chini, R. 1981, *Astr. Ap.*, **99**, 346.
 Cohen, M. 1980, *M.N.R.A.S.*, **191**, 499.
 ———. 1983, *Ap. J. (Letters)*, **270**, L69.
 ———. 1984, *Phys. Rept.*, **116**(4), 173.
 Cohen, M., Emerson, J. P., and Beichman, C. 1989, *Ap. J.*, **339**, 455 (CEB).
 Cohen, M., Harvey, P. M., and Schwartz, R. D. 1985, *Ap. J.*, **296**, 633.
 Cohen, M., and Kuhl, L. V. 1979, *Ap. J. Suppl.*, **41**, 743.
 Cohen, M., and Schwartz, R. D. 1976, *M.N.R.A.S.*, **174**, 137.
 Duncan, W. D., Robson, E. I., Ade, P. A. R., Griffin, M. J., and Sandell, G. 1989, *M.N.R.A.S.*, submitted.
 Draine, B. T. 1989, in *Infrared Spectroscopy in Astronomy*, ed. B. H. Kaldeich (Noordwijk: ESA), p. 93.
 Draine, B. T., and Lee, H. M. 1984, *Ap. J.*, **285**, 89.
 Dyck, H. M., Simon, T., and Zuckerman, B. 1982, *Ap. J. (Letters)*, **255**, L103.
 Edwards, S., Cabrit, S., Strom, S. E., Heyer, I., and Strom, K. M. 1987, *Ap. J.*, **321**, 473.
 Elsasser, H., and Staude, H. J. 1978, *Astr. Ap.*, **70**, L3.
 Emerson, J. P. 1988, in *Formation and Evolution of Low Mass Stars*, ed. A. K. Dupree and M. T. V. T. Lago (Dordrecht: Kluwer), p. 21.
 Gledhill, T. M., and Scarrott, S. M. 1989, *M.N.R.A.S.*, **236**, 139.
 Grasdalen, G., Strom, S., Strom, K., Capps, R., Thompson, D., and Castalez, M. 1984, *Ap. J. (Letters)*, **283**, L57.
 Griffin, M. J., Ade, P. A. R., Orton, G. S., Robson, E. I., Gear, W. K., Nolt, I. G., and Radostitz, J. V. 1986, *Icarus*, **65**, 244.
 Hartmann, L., and Kenyon, S. J. 1987, *Ap. J.*, **312**, 243.
 Hartmann, L., and Raymond, J. C. 1989, preprint.
 Harvey, P. M., Thronson, H. A., and Gatley, I. 1979, *Ap. J.*, **231**, 115.
 Herbig, G. H., and Bell, K. R. 1988, *Lick Obs. Bull.*, No. 1111.
 Hildebrand, R. H. 1983, *Quart. J.R.A.S.*, **24**, 267.

- Keene, J., and Masson, C. R. 1990, preprint.
- Kenyon, S. J., and Hartmann, L. 1987, *Ap. J.*, **323**, 714.
- Leinert, C. and Hass, M. 1989, *Ap. J. (Letters)*, **342**, L39.
- Lin, D. N. C., and Pringle, J. E. 1990, preprint.
- Lynden-Bell, D., and Pringle, J. E. 1974, *MN.R.A.S.*, **168**, 603.
- Mendoza, E. E. V. 1966, *Ap. J.*, **143**, 1010.
- . 1968, *Ap. J.*, **151**, 977.
- Myers, P. C., Fuller, G. A., Mathieu, R. D., Beichman, C. A., Benson, P. J., Schild, R. E., and Emerson, J. P. 1987, *Ap. J.*, **319**, 340.
- Orton, G. S., Griffin, M. J., Ade, P. A. R., Nolt, I. G., and Radostitz, J. V., Robson, E. I., and Gear, W. K. 1986, *Icarus*, **67**, 289.
- Purcell, E. M. 1969, *Ap. J.*, **158**, 433.
- Rucinski, S. M. 1985, *A.J.*, **90**, 2321.
- Rydgren, A. E., Schmeltz, J. T., and Vrba, F. J. 1982, *Ap. J.*, **256**, 168.
- Rydgren, A. E., Schmeltz, J. T., Zak, D. S., and Vrba, F. J. 1984, *Broad Band Spectral Energy Distributions of T Tauri Stars in the Taurus-Auriga Region* (Pub. US Naval Obs., Vol. XXV, Part I).
- Rydgren, A. E., Strom, S. E., and Strom, K. M. 1976, *Ap. J. Suppl.*, **30**, 307.
- Rydgren, A. E., and Vrba, F. J. 1981, *A.J.*, **86**, 725.
- Rydgren, A. E., and Vrba, F. J. 1983, *A.J.*, **88**, 1017.
- Rydgren, A. E., and Zak, D. S. 1987, *Pub. A.S.P.*, **99**, 141.
- Sargent, A. I., and Beckwith, S. 1987, *Ap. J.*, **323**, 294.
- Shu, F. H., Adams, F. C., and Lizano, S. 1987, *Ann. Rev. Astr. Ap.*, **25**, 23.
- Strom, K. M., Strom, S. E., Edwards, S., Cabrit, S., and Strutskie, M. F. 1989, *A.J.*, **97**, 1451.
- Strom, S. E., Strom, K. M., Kenyon, S. J., and Hartmann, L. 1988, *A.J.*, **95**, 534.
- Strom, S. E., Strom, K. M., and Vrba, F. J. 1976, *A.J.*, **81**, 320.
- Terebey, S., Shu, F. H., and Cassen, P. 1984, *Ap. J.*, **286**, 529.
- Tielens, A. G. G. M., and Allamandola, L. J. 1987, in *Interstellar Processes*, ed. D. Hollenbach and H. Thronson (Dordrecht: Reidel), p. 397.
- Vrba, F. J., Rydgren, A. E., and Zak, D. S. 1985, *A.J.*, **90**, 2074.
- Weintraub, D. A., Sandell, G., and Duncan, W. D. 1989, *Ap. J. (Letters)*, **340**, L69 (WSD).
- Wilking, B. A., and Lada, C. J. 1983, *Ap. J.*, **274**, 698.
- Woody, D. P., Scott, S. L., Scoville, N. Z., Mundy, L. G., Sargent, A. I., Padin, S., Tinney, C. G., and Wilson, C. D. 1989, *Ap. J. (Letters)*, **337**, L41.
- Wright, E. L. 1976, *Ap. J.*, **210**, 250.
- . 1987, *Ap. J.*, **320**, 818.

FRED C. ADAMS and GARY A. FULLER: Harvard-Smithsonian Center for Astrophysics, 60 Garden Street, Cambridge, MA 02138

JAMES P. EMERSON: Physics Department, Queen Mary and Westfield College, Mile End Road, London, E1 4NS, England, UK